COMMUNICATION

Low-Cost, Flexible, and Self-Cleaning 3D Nanocone Anti-Reflection Films for High-Efficiency Photovoltaics

Kwong-Hoi Tsui, Qingfeng Lin, Hungtao Chou, Qianpeng Zhang, Huiying Fu, Pengfei Qi, and Zhiyong Fan*

A photovoltaic device is essentially a solar-energy harvesting device, converting the incoming photons to charge carriers. Therefore, the capability of capturing the incident photons is one of the key characteristics of a solar cell device. Since the reflectance loss of light leads to inefficient utilization of the incident photons, various anti-reflection (AR) schemes have been developed to achieve high-efficiency solar cell devices. Conventionally, quarter-wavelength ($\lambda/4$) AR coatings have been widely used on the front surface of photovoltaic devices/modules.[1] However, their effectiveness typically has wavelength and incident-angle dependencies, and high-quality AR coating relies on chemical or physical deposition processes that increase the production cost.[2–4] Meanwhile, nano/microstructures have been discovered with broadband light trapping capability, which can significantly suppress device front-surface reflection.[5,6] Hence, a variety of nano/microstructures, such as nano/micro-pyramids,[7–9] nanowires,[10–12] nanopillars (NPLs),[13–15] nanocones (NCs),[16–18] nanodomes,[19] nanospheres,[20–22] and so forth, have been extensively studied with different photonic materials, such as Si, Ge, CdS, and Cu(In, Ga)Se (CIGS). Although these structures have demonstrated appealing performance on photon management, many of them have been fabricated with costly and/or destructive methods, such as lithographic and wet/dry etching approaches.[8,23] And these approaches may not be necessarily applicable for thin-film photovoltaics, especially for flexible applications. On the other hand, fabricating active photovoltaic materials into nano/microstructures introduces defects and the increased surface recombination, hence it needs to be carefully designed and performed.[10,24–26] In this work, we have utilized a facile molding process to fabricate flexible plastic AR films with three-dimensional (3D) nanocone arrays on the front surface. The geometry of the nanocones, i.e., their pitch and height, can be precisely controlled by tuning the structure of the inverse nanocone mold fabricated with anodization in conjunction with nanoimprinting. The AR films can be readily attached to flat substrates, such as glass

and Si, without adhesive glue. Therefore, their effectiveness has been examined on high-efficiency CdTe thin-film solar cells fabricated on glass substrates. The optical reflectance measurements and simulations have shown that the nanocone structure can significantly reduce the reflectance of the glass window above the CdTe light-absorbing layer, resulting in appreciable device performance improvement, confirmed by both current–voltage characteristics and quantum efficiency measurements. Furthermore, it was found that the improved AR effect can be observed with oblique light incident angle, which is highly beneficial for practical deployment of photovoltaic panels. Particularly for the studied high performance CdTe solar cell devices, it was found that over 1 kW h m^{-2} daily electrical energy output can be achieved with the nanocone AR film, indicating ca. 7% overall enhancement over the same device without the nanocone AR film. Besides the intriguing AR property, it was also discovered that the nanocone structures are superhydrophobic, with a high water contact angle. This effect suggests the plastic AR film can possess a self-cleaning function, which is favorable for solar cells/modules deployed in dusty environments.

The flexible nanocone films in this work were fabricated by molding polydimethylsiloxane (PDMS) with anodic alumina inverse-nanocone (i-cone) arrays fabricated on aluminium (Al) substrates. Note that PDMS is a low cost, environmental friendly, and highly transparent material. On the other hand, other plastic materials, such as polycarbonate, polyimide, etc., can also be molded with a similar approach to satisfy various practical requirements, such as flexibility, durability, etc.[27] **Figure 1**a1 to a3 shows schematics of the fabrication process. Briefly, an electrochemically polished-clean Al foil was imprinted using a silicon stamp with hexagonally ordered nanopillars with height of 200 nm and tunable pitch of 500 nm to 2 µm to produce a nanoindentation array on the surface of the Al foil, as shown in Figure 1a1. Thereafter, the i-cone array (Figure 1a2) was fabricated by a multi-step anodization and wet etching process on the imprinted Al foil in an acidic solution with a proper direct-current (DC) voltage.[27–29] Figure 1b and the inset show scanning electron microscopy (SEM) images of a fabricated i-cone array with cross-sectional and top views, respectively. Note that both of the pitch and the height of the i-cones shown in Figure 1b are 1 µm, however, it is largely tunable, as we reported previously.[27] After obtaining an alumina i-cone array, a 50 nm Au film was sputtered on the surface of it as an anti-sticking layer between the i-cone array and PDMS for easy peeling off of PDMS from the template subsequently, so that the template can be reused multiple times without leaving PDMS residue. Finally, the premixed PDMS (Sylgard 184, Dow Corning 10:1 ratio with the curing agent) was poured onto the Au-coated template followed by a degas and curing process at
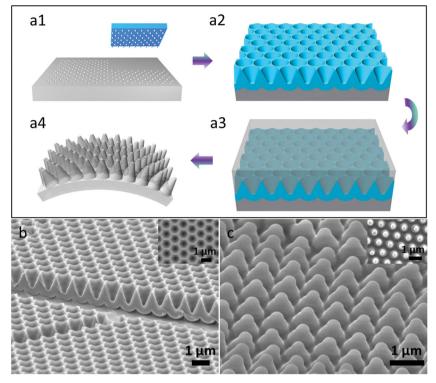
K.-H. Tsui,[+] Q. F. Lin,[+] Q. P. Zhang,
Dr. H. Y. Fu, Prof. Z. Y. Fan
Department of Electronic and Computer Engineering
The Hong Kong University of Science and Technology
Clear Water Bay, Kowloon, Hong Kong, China SAR
E-mail: eezfan@ust.hk
Dr. H. T. Chou, Dr. P. F. Qi
Clean Energy International
46535 Fremont Blvd, Fremont, CA 94538, USA
[+]These authors contribute equally to this work.

Figure 1. Schematics of nanocone film and SEM images of Au-coated template and PDMS nanocone. a1) A Si mold with hexagonally ordered nanopillars used as imprint mold with four nanoimprint steps. a2) The i-cone array fabricated by a multi-step anodization and wet etching process on the imprinted Al foil. a3) Premixed PDMS poured on Au-coated template followed by a degas and curing process. a4) Regular nanocone on flexible PDMS after peeling off. b) Au-coated template with 1 μm pitch and 1 μm depth. c) Nanocone with 1 μm pitch and 1 μm depth.

substrates without using other adhesives.[30] This self-attachable property leads to convenient mounting and replacement of the nanocone AR film on a solar cell surface. In this work, we have examined the effectiveness of nanocone AR film on high efficiency CdTe solar cells. Figure 2b schematically illustrates the structure of the solar cell device with nanocone PDMS film attached on the top. The details of the CdTe solar cell fabrication can be found in the Supporting Information; briefly, the CdTe solar cells were fabricated on fluorine-doped tin oxide glass. A layer of *n*-type CdS window layer was deposited using chemical bath deposition. Then, multicrystalline *p*-type CdTe film was deposited with close space sublimation followed by proper $CdCl_2$ treatment and annealing. Then a layer of Mo/Al stack was evaporated on the back side of the device with a shadow mask serving as the back contact. In the Supporting Information, Figure S2 shows the cross-sectional SEM image of the completed CdTe solar cell. Figure 2c shows the visual effect of the nanocone AR layer on CdTe devices captured under a "reflection mode". The bare sample on the right shows the clear reflection of the indoor fluorescence lamp. In contrast, the sample with PDMS nanocone on the left conspicuously shows the suppression of the reflectance. The detailed optical and device

80 °C, as shown in Figure 1a3. Afterwards, a PDMS nanocone film with thickness ca. 0.2 mm was obtained by directly peeling off PDMS from i-cone template, as demonstrated in Figure 1a4 and c. Notably, the nanoimprint process is a much more efficient process to fabricate nanoindentations as compared to lithographic processes. It can be repetitively performed on one Al substrate at different locations, hence a large-scale i-cone array can be conveniently obtained. In the Supporting Information, Figure S1 shows a photograph of an i-cone array sample obtained with four nanoimprint steps.

Following the process described above, the obtained nanocone PDMS films have a number of distinct features that make them attractive as AR layers. **Figure 2**a shows a photograph of a fabricated nanocone film naturally attached on a 0.18 mm thick polycarbonate film, which demonstrates its excellent flexibility. Note that the nanocones are in the middle of the sample, showing a diffraction effect indicating their excellent regularity. Due to the strong Van der Waals interaction between PDMS and glass, PDMS can be easily and firmly attached to flat glass
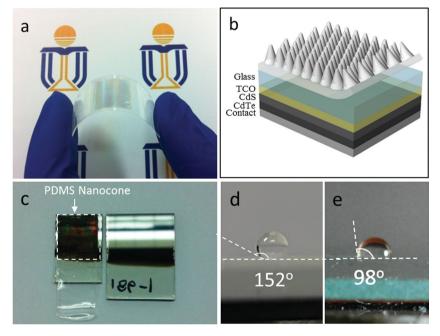

Figure 2. a) Flexible nanocone film. b) Schematic structure of the solar cell device with nanocone PDMS film attached on the top. c) Visual effect of the nanocone AR layer on CdTe devices. The bare sample on the right and the sample with PDMS nanocone on top on the left. d) A drop of water on the nanocone PDMS film showing a large contact angle of 152°. e) A drop of water on the flat PDMS film showing a contact angle of 98°.

performance characterization will be discussed later. In addition to the AR property, it was also found that the PDMS nanocone arrays have superhydrophobic characteristic with large water contact angle. As illustrated in Figure 2d, a 2 μL water droplet was placed on the surface of the nanocone PDMS film and the contact angle was found to be 152°. In comparison, the contact angle on a flat PDMS film was also measured, as shown in Figure 2e, and found to be 98°; this clearly demonstrates the improvement of hydrophobicity with nanocone structure. In fact, it has been reported that fabricating hydrophobic materials into nanostructure can largely increase water contact angle.[19] Superhydrophobicity and the "Lotus effect" have been extensively investigated for self-cleaning surfaces.[31–34] In the Supporting Information video, it can be seen that water dripped down does not stay on the nanocone film, which can lead to easy dust removal. This unique property of PDMS nanocones suggests that, in addition to the AR capability, the nanocone film also has attractive self-cleaning function for solar cells/modules deployed in dusty environments.

To quantitatively characterize the AR effect of 3D PDMS nanocones on CdTe photovoltaic devices, reflectance spectra in a wavelength range from 400 to 900 nm were obtained using a home-built ultraviolet/visible measurement set up. Note that due to the light-scattering nature of the 3D nanostructures, an integrating sphere was used to acquire the reflected light accurately.[29] **Figure 3**a shows the reflectance spectra of a bare CdTe device and a device covered with a 3D nanocone AR film measured with normal incident light. Note that both of the pitch

and the height of the nanocones are 1 μm. It can be seen that the reflectance of the device with the nanocone AR film was decreased by ca. 4% for the given wavelength range, as compared to the one without PDMS nanocones. This reduction of front-side reflectance is primarily due to the tapered nanocone shape, which provides a gradual change of effective refractive index from air to PDMS.[35–37] In addition, since there is marginal difference on refractive index ($n = 1.41$ at $\lambda = 550$ nm) for PDMS and the underneath glass ($n = 1.46$ at $\lambda = 550$ nm), the reflectance at the PDMS/glass interface is negligible. There is still a few-percent reflectance after using the nanocone AR film, which originates from the layers below, including FTO ($n = 1.92$ at $\lambda = 550$ nm), CdS ($n = 2.51$ at $\lambda = 550$ nm), and CdTe ($n = 3.05$ at $\lambda = 550$ nm). Further elimination of device reflection can be achieved by roughening the back side of glass substrate by wet etching before FTO coating to further suppress the reflectance from these underneath layers.

In order to verify the reflectance spectra obtained from the experiments and further shed light on how the light couples into nanocones, finite-difference-time-domain (FDTD) simulations of reflectance spectra and the cross-sectional electric field intensity ($|E|^2$) distribution of electromagnetic wave at 600 nm wavelength were obtained with and without nanocone structure, as illustrated in Figure 3b. The overall trend of simulated reflectance spectra is quite consistent with that of the experimental ones, with apparent reduction of reflectance for nanocones. Meanwhile, the oscillations of the spectra can be attributed to the interference between the top glass–air interface and bottom
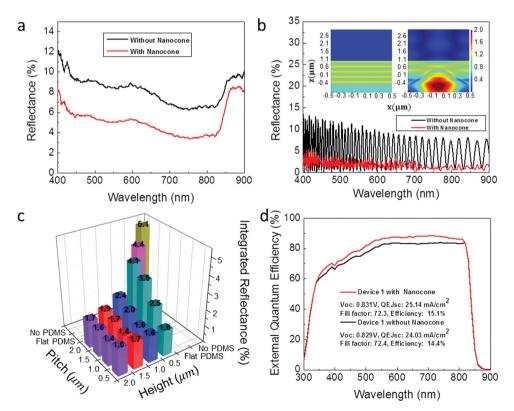

Figure 3. a) Reflectance measurements of CdTe device 1 with and without PDMS nanocone film. b) FDTD simulations of reflectance spectra and the cross-sectional electric field intensity distribution of electromagnetic wave at 600 nm wavelength. c) Simulated integrated reflectance at different pitches and heights. d) QE measurement of CdTe device 1 with and without PDMS nanocone film.

COMMUNICATION

glass–FTO interface. This is not seen in the experimental reflectance spectra due to the non-ideally planar glass surfaces in reality. Additionally, reflectance spectra with different PDMS thicknesses have been simulated, as shown in the Supporting Information, Figure S3, demonstrating that the overall reflectance of CdTe device with 3D nanocone film is not sensitive to the thickness of PDMS layer. In the cross-sectional electric field intensity ($|E|^2$) distribution shown in the inset of Figure 3b, the electromagnetic (EM) plane waves propagate downwards from $Z = 1$ µm. For the left inset, the top surface of the glass substrate locates at $Z = -0.5$ µm. And for the right inset, the top of the nanocone locates at $Z = 0.5$ µm. Note that the color index at the specific location reflects the intensity of $|E|^2$ at that point, normalized with the EM source propagating in free space. The yellow stripe-like patterns indicate interference between the incoming wave with the reflected wave. And the color above $Z = 1$ µm manifests the intensity of the reflected wave. It can be seen that the existence of nanocones results in weaker interference and weaker intensity of the reflected wave. In addition, it can conspicuously be seen from the $|E|^2$ distribution inside the nanocone structure that the EM wave energy can be efficiently coupled into the nanocone.

It has been reported in a few studies that the geometry of the nanostructures can affect their photon-management properties.[29,38] As mentioned before, the geometric factors of nanocones, i.e. pitch and height, can be largely tuned with the established approach. Therefore, systematic optical simulations have been performed in order to identify the optimal structures for light trapping. Particularly, the reflectance spectra of nanocones with different pitches and heights were simulated to investigate the influence of their geometry on the AR effect. These spectra were then integrated with AM1.5G photon flux spectrum to obtain the total integrated reflectance.[28] As shown in Figure 3c, all the nanocone structures demonstrate lower reflectance than bare glass (no PDMS) and PDMS without nanocones. Furthermore, the integrated reflectance does depend on the geometry of the nanocones. Overall, reflectance decreases when increasing nanocone height at a fixed pitch, or reducing pitch at fixed height. These interesting trends can be explained with the following rationale. Due to the conical shape of the individual nanostructures, both height increase with the fixed pitch and pitch decrease with the fixed height leads to steeper conical side wall slope. This can result in more probability of light scattering between nanocones, thus suppressing reflectance. Most importantly, these simulations confirm that the PDMS nanocones with 1 µm pitch and 1 µm height obtained in the experiments have almost the optimal AR effect.

The purpose of introducing optical AR effect on solar cells is to improve photon utilization efficiency, eventually to enhance device performance. Therefore, CdTe solar-cell device electrical characterization was performed systematically with and without attaching the nanocone AR film for the sake of comparison. Figure 3d shows the external quantum efficiency (QE) measurements (Oriel QE-PV-SI, Newport Corporation) of one CdTe solar cell device with and without a nanocone AR film, which provides direct evidence of the AR effect. After integrating with the AM 1.5G spectrum, the short-circuit current density (QEJ_{sc}) of devices with and without nanocones were obtained as 25.14 and 24.03 mA cm^{-2}, respectively, which indicates ca.

4.6% enhancement. Meanwhile, the current density–voltage (J–V) curve of the device with and without the nanocone AR film was also acquired with an solar simulator (Newport corporation, 91150V) under 1 Sun illumination, as shown in the Supporting Information, Figure S4a. With the obtained open-circuit voltage (V_{oc}), fill factor (FF), and QEJ_{sc}, the power conversion efficiencies of the device with and without nanocones were calculated as 15.1% and 14.4%, respectively, as shown in the inset of Figure 3d. These results demonstrate ca. 4.9% improvement of conversion efficiency, which is substantial for a high-performance CdTe solar cell device. As a matter of fact, in order to obtain a credible trend, three devices were measured using the same nanocone AR film since it can be easily detached and placed on any device. The J–V curves and QE curves are shown in the Supporting Information, Figure S4 and S5, and the measured parameters of all three devices are summarized in Table S1, which consistently show the improvement of J_{sc} and marginal improvement of V_{oc}. Note that in these cases QEJ_{sc} were used for calculation of efficiency instead of the J_{sc} directly obtained from the solar simulator due to their better accuracy. As discussed above, the nanocone AR structure reported here does not introduce defects and extra surface area on the active photovoltaic material, thus does not lead to a drop of V_{oc}, as encountered in other cases. Note that the current world-record J_{sc} for CdTe solar cell is 28.59 mA cm^{-2};[39] the obtained QEJ_{sc} here is not too far from this value. Research has shown that for high-efficiency solar cells, even marginal improvement on one of the figure-of-merits is challenging. For a close-to-optimal photovoltaic device, there is a delicate balance between light capturing and photocarrier collection, and an aggressive approach to improve one of them by altering device structure may lead to loss on the other one if not designed properly. In this regard, introducing an additional AR film on top of the device can conveniently improve its performance without sabotaging the balance between the light absorption and photocarrier dynamics in the device.

It is worth pointing out that the above measurements were carried out with normal incident light, while for practical operation, the angle of solar irradiation changes over the time in a day. Therefore, light absorption for angular incidence should be investigated. In our experiments, the reflectance of a CdTe device with and without PDMS nanocones were obtained for light incident angles from 0° (normal incidence) to 60° in 10° intervals using an integrating sphere and a broadband halogen light source, as shown in **Figure 4**a. Intriguingly, it can be clearly seen that the reflectance of a nanocone device remains unchanged at ca. 5% for incident angles from 0° to 60°. However, it increases progressively from 8.5% up to 13.2% when the incident angle is increased to 60° without nanocone film. This observation suggests that the nanocone AR effect is even more pronounced at higher incident angle. Furthermore, J_{sc} at different incident angles were also measured and shown in Figure 4b, with V_{oc}, FF, and conversion efficiency shown in the Supporting Information, Table S2. Apparently from Figure 4b, the absolute enhancement of J_{sc} is approximately 0.8 to 1.1 mA cm^{-2} and is rather independent from incident angle. Nevertheless, due to the reduction of J_{sc} when increasing the angle, the relative improvement of J_{sc} progressively increases from 3.6% to 8.5% when the incident angle increases from 0° to 60°. Besides,
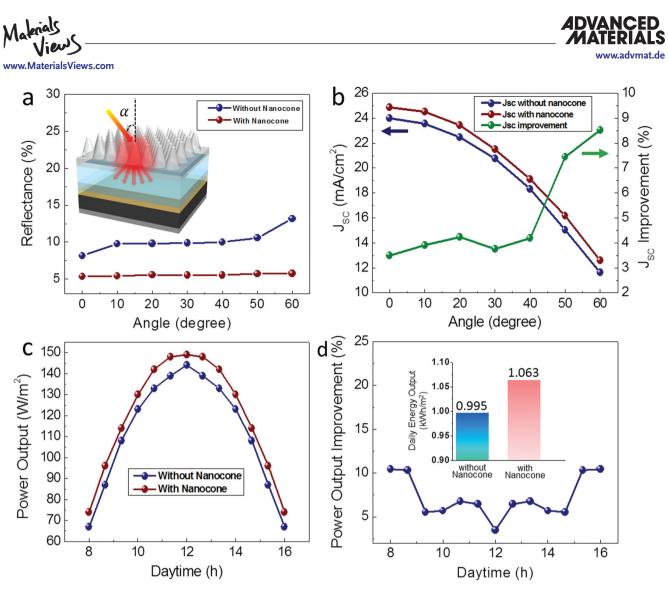
Figure 4. a) Reflectance spectra of a CdTe device with and without PDMS nanocone film obtained for the light incident angles tuning from 0° (normal incident) to 60° at 10° intervals. b) J_{sc} of a CdTe device with and without PDMS nanocone film obtained at different incident angles, together with the angular-dependent relative improvement of J_{sc}. c) Power output of a CdTe device with and without PDMS nanocone film against daytime. d) Power output improvement of a CdTe device with and without PDMS nanocone film against daytime, with their daily energy output in the inset.

it can be also seen from Supporting Information Table S2 that V_{oc} increases with incident angle as well. Note that J_{sc} from the solar simulator was used for efficiency calculation due to the difficulty on integrating the tilt setup with the QE system. Since the light source of the solar simulator is collimated, tilting the solar cell device away from normal incidence results in reduction of the project area that receives light; therefore the real efficiency of the device, which is defined as the ratio between the electrical power output and the actual optical power input, needs to be calibrated with area reduction, as shown in the values inside the brackets in Supporting Information Table S2. The calibrated efficiencies in Supporting Information Table S2 more clearly show the advantage of the nanocone AR film at higher incident angle. Particularly the efficiency of the device is improved by ca. 10% for 60° incident angle. This is of significance for practical deployment of solar panels without a costly solar tracking system. To further evaluate this point, power output of the device is plotted against daytime in a day assuming normal incidence, corresponding to noon time, and

60°, corresponding to 4 h away from noon time.[37] As shown in Figure 4c, the nanocone device demonstrates an all-day improvement of electrical power output, with the percentage showing in Figure 4d. With these results, daily energy output can be readily calculated and shown in the inset of Figure 4d, with the detail of the calculations shown in the Supporting Information (Figure S6). Interestingly, the solar cell device with the nanocone AR film demonstrates 1.063 kW h m^{-2} daily energy output, which has close to 7% enhancement over the device without the AR film.

In summary, we have demonstrated a facile process to fabricate flexible nanocone arrays with well-engineered nanotemplates. The flexible nanocone film can be easily attached to a flat substrate, such as glass, Si or a flexible substrate, without addition of any adhesive glue. The 3D nanocone films have been used as an additional AR layer mounted on high efficiency CdS/CdTe solar cells in this work. The film was found to be superhydrophobic with self-cleaning function. More importantly, the optical property investigations have shown that the

COMMUNICATION

nanocone structure can significantly reduce the device front-side reflectance, which was verified by FDTD simulation. The systematic solar cell device electrical characterizations clearly and consistently showed that the nanocone AR film can considerably improve device short-circuit current density with marginal improvement on open-circuit voltage, leading to a conspicuous increase of power conversion efficiency. Intriguingly, it was discovered that the AR effectiveness improves with light incident angle, leading to substantial enhancement of daily electrical energy output over 1 kW h m^{-2}. Notably, this type of flexible AR film can be applied for a wide range of photovoltaic technologies based on rigid and flexible substrates, including Si- and copper–indium–gallium–selenide-based technologies. Other polymeric materials, such as those with high refractive index, could be also used instead of PDMS if the AR films will be mounted on high-refractive photovoltaic materials to achieve better AR effect. Overall, the process demonstrated here is highly versatile and it enables a new route to fabricate cost-effective AR layers.

Experimental Section

Materials: Aluminium foil (0.25 mm thick, 99.99% purity) was purchased from Alfa Aesar, polycarbonate film (0.2 mm thick) was provided by Suzhou Zhuonier Optical Materials Co., Ltd., silicone elastomer and the curing agent were obtained from Dow Corning. FTO glass substrate (Pilkington TEC10 Glass) was purchased from Pilkington. All other chemicals were products of Sigma-Aldrich.

Flexible Nanocone Films Assembly: An electrochemically polished clean Al foil was imprinted using a silicon stamp with hexagonally ordered nanopillars with height of 200 nm and tunable pitch of 500 nm to 2 µm to produce a nanoindentation array on the surface of the Al foil. Thereafter, the i-cone array was fabricated by a multi-step anodization and wet etching process on the imprinted Al foil in an acidic solution with a proper direct-current (DC) voltage.[27–29] Afterwards, a 50 nm Au film was sputtered on the surface of the obtained alumina i-cone array as an anti-sticking layer between the i-cone array and PDMS for easy peeling off of PDMS from the template subsequently. Finally, the premixed PDMS (Sylgard 184, Dow Corning 10:1 ratio with the curing agent) was poured onto the Au-coated template followed by a degas and curing process at 80 °C. Afterwards, a PDMS nanocone film with thickness ca. 0.2 mm was obtained by directly peeling off PDMS from i-cone template.

Fabrication of CdTe Solar Cell Devices: The CdTe solar cells were fabricated on fluorine-doped tin oxide glass. A layer of *n*-type CdS window layer was deposited using chemical bath deposition. Then, multicrystalline *p*-type CdTe film was deposited with close space sublimation followed by proper CdCl$_2$ treatment and annealing. In the end, a layer of Mo/Al stack was evaporated on the back side of the device with a shadow mask serving as the back contact.

Device Characterization: SEM images of Au-coated samples were characterized by a JEOL JSM-6700F SEM working at 5 kV. UV-vis spectra of all devices were obtained using a home-built ultraviolet/visible measurement set up. The QE measurements of CdTe solar cells were achieved by Oriel QE-PV-SI (Newport Corporation). All the *J–V* curves were carried out using a solar simulator (Newport corporation, 91150V) under 1 Sun illumination.

Supporting Information

Supporting Information is available from the Wiley Online Library or from the author.

[1] The Physics of Solar Cells (Ed: J. Nelson), Imperial College Press, London **2003**.

[2] K. Ramanathan, M. A. Contreras, C. L. Perkins, S. Asher, F. S. Hasoon, J. Keane, D. Young, M. Romero, W. Metzger, R. Noufi, *Prog. Photovoltaics Res. Appl.* **2003**, *11*, 225.

[3] B. Richards, *Prog. Photovoltaics Res. Appl.* **2004**, *12*, 253.

[4] S. Chhajed, M. F. Schubert, J. K. Kim, E. F. Schubert, *Appl. Phys. Lett.* **2008**, *93*, 251108.

[5] B. Hua, Q. Lin, Q. Zhang, Z. Fan, *Nanoscale* **2013**, *5*, 6627.

[6] R. Yu, Q. Lin, S. F. Leung, Z. Fan, *Nano Energy* **2012**, *1*, 57.

[7] S. E. Han, G. Chen, *Nano Lett.* **2010**, *10*, 4692.

[8] A. Mavrokefalos, S. E. Han, S. Yerci, M. S. Branham, G. Chen, *Nano Lett.* **2012**, *12*, 2792.

[9] W. Wei, M. Tsai, S. Ho, S. Tai, C. Ho, S. Tsai, C. Liu, R. Chung, J. He, *Nano Lett.* **2013**, *13*, 3658.

[10] E. Garnett, P. Yang, *Nano Lett.* **2010**, *10*, 1082.

[11] H. Chang, K. Lai, Y. Dai, H. Wang, C. Lin, J. He, *Energ. Environ. Sci.* **2011**, *4*, 2863.

[12] E. C. Garnett, M. L. Brongersma, Y. Cui, M. D. McGehee, *Annu. Rev. Mater. Res.* **2011**, *41*, 269.

[13] Z. Y. Fan, R. Kapadia, P. W. Leu, X. B. Zhang, Y. L. Chueh, K. Takei, K. Yu, A. Jamshidi, A. A. Rathore, D. J. Ruebusch, M. Wu, A. Javey, *Nano Lett.* **2010**, *10*, 3823.

[14] Z. Y. Fan, H. Razavi, J. W. Do, A. Moriwaki, O. Ergen, Y. L. Chueh, P. W. Leu, J. C. Ho, T. Takahashi, L. A. Reichertz, S. Neale, K. Yu, M. Wu, J. W. Ager, A. Javey, *Nat. Mater.* **2009**, *8*, 648.

[15] R. Kapadia, Z. Fan, A. Javey, *Appl. Phys. Lett.* **2010**, *96*, 103116.

[16] J. Zhu, Z. F. Yu, G. F. Burkhard, C. M. Hsu, S. T. Connor, Y. Q. Xu, Q. Wang, M. McGehee, S. H. Fan, Y. Cui, *Nano Lett.* **2009**, *9*, 279.

[17] B. Wang, P. W. Leu, *Nanotechnology* **2012**, *23*, 194003.

[18] K. X. Wang, Z. Yu, V. Liu, Y. Cui, S. Fan, *Nano Lett.* **2012**, *12*, 1616.

[19] J. Zhu, C. Hsu, Z. Yu, S. Fan, Y. Cui, *Nano Lett.* **2010**, *10*, 1979.

[20] J. Grandidier, D. M. Callahan, J. N. Munday, H. A. Atwater, *Adv. Mater.* **2011**, *23*, 1272.

[21] X. Lai, J. E. Halpert, D. Wang, *Energy Environ. Sci.* **2012**, *5*, 5604.

[22] Y. Yao, J. Yao, V. K. Narasimhan, Z. Ruan, C. Xie, S. Fan, Y. Cui, *Nat. Commun.* **2012**, *3*, 664.

[23] M. D. Kelzenberg, S. W. Boettcher, J. A. Petykiewicz, D. B. Turner-Evans, M. C. Putnam, E. L. Warren, J. M. Spurgeon, R. M. Briggs, N. S. Lewis, H. A. Atwater, *Nat. Mater.* **2010**, *9*, 239.

[24] C. M. Hsu, C. Battaglia, C. Pahud, Z. Ruan, F. J. Haug, S. Fan, C. Ballif, Y. Cui, *Adv. Energy Mater.* **2012**, *2*, 628.

[25] S. Jeong, E. C. Garnett, S. Wang, Z. Yu, S. Fan, M. L. Brongersma, M. D. McGehee, Y. Cui, *Nano Lett.* **2012**, *12*, 2971.

[26] S. Tsai, H. Chang, H. Wang, S. Chen, C. Lin, S. Chen, Y. Chueh, J. He, *ACS Nano* **2011**, *5*, 9501.

[27] Q. Lin, S. Leung, K. Tsui, B. Hua, Z. Fan, *Nanoscale Res. Lett.* **2013**, *8*, 268.

[28] Q. Lin, B. Hua, S. Leung, X. Duan, Z. Fan, *ACS Nano* **2013**, *7*, 2725.

[29] S. F. Leung, M. Yu, Q. Lin, K. Kwon, K. L. Ching, L. Gu, K. Yu, Z. Fan, *Nano Lett.* **2012**, *12*, 3682.

[30] A. Galliano, S. Bistac, J. Schultz, *J. Colloid Interface Sci.* **2003**, *265*, 372.

[31] B. Bhushan, Y. C. Jung, K. Koch, *Langmuir* **2009**, *25*, 3240.

[32] V. A. Ganesh, H. K. Raut, A. S. Nair, S. Ramakrishna, *J. Mater. Chem.* **2011**, *21*, 16304.

[33] K. Koch, B. Bhushan, W. Barthlott, *Soft Matter* **2008**, *4*, 1943.

[34] Self-Cleaning Materials and Surfaces: A Nanotechnology Approach (Ed: W. A. Daoud), John Wiley & Sons, Ltd, United Kingdom **2013**.

[35] L. K. Yeh, K. Y. Lai, G. J. Lin, P. H. Fu, H. C. Chang, C. A. Lin, J. H. He, *Adv. Energy Mater.* **2011**, *1*, 506.

[36] Y. L. Chueh, Z. Y. Fan, K. Takei, H. Ko, R. Kapdia, A. Rathore, N. Miller, K. Yu, M. Wu, E. E. Haller, A. Javey, *Nano Lett.* **2010**, *10*, 520.

[37] R. Yu, K. Ching, Q. Lin, S. Leung, D. Arcrossito, Z. Fan, *ACS Nano* **2011**, *5*, 9291.

[38] V. K. Narasimhan, Y. Cui, *Nanophotonics* **2013**, *2*, 187.

[39] M. A. Green, K. Emery, Y. Hishikawa, W. Warta, E. D. Dunlop, *Prog. Photovoltaics Res. Appl.* **2013**, *21*, 827.

COMMUNICATION